High Resolution Electron Microscopy of Low Temperature Silver- and Gold/Silver-Selenide, Au[x]Ag_[x]Se (x=0-0.5) (Commemoration Issue Dedicated to Professor Natsu Uyeda, on the Occasion of His Retirment)

AUTHOR(S):

Günter, John R.; Keusch, Paul

Bull. Inst. Chem. Res., Kyoto Univ., Vol. 66, No. 5, 1988

High Resolution Electron Microscopy of Low Temperature Silver- and Gold/Silver-Selenide, $Au_xAg_{2-x}Se$ ($x=0$–0.5)

John R. GÜNTER and Paul KEUSCH

Received September 6, 1988

HREM observations on thin films of Low Temperature Ag_2Se reveal the coexistence of various phases, while the presence of gold in thin $Au_xAg_{2-x}Se$ films, prepared by reaction of epitaxial Au/Ag films with Se vapour, seems to stabilize the tetragonal cell only. Observed HREM and simulated images combined with optical diffraction and arguments on bond lenghts allow the deduction of a structural model for this phase: Monoclinic pseudotetragonal, S.G. P2, $a=c=0.706$ nm, $b=0.498$ nm, $\beta=90°$, $Z=4$, atomic positions: Se in 0, 0, 0; 1/2, 1/2, 0; 1/2, 0, 1/2; 0, 1/2, 1/2; Ag in 0.84, 0, 0.34; 0.16, 0, 0.66; 0.3, 0.25, 0.25; 0.7, 0.25, 0.75; 0.36, 0.5, 0.64; 0.64, 0.5, 0.36; 0.2, 0.75, 0.25; 0.8, 0.75, 0.25.

KEY WORDS: Silver selenide/ Gold-Silver-Selenide/ Topotactic reaction/

INTRODUCTION

Silver selenide (Ag_2Se) undergoes a first order polymorphic transition at 133°C[1]. Above the transition temperature the high-temperature (HT) phase behaves as a metal and its structure, first determined by Ralphs[2], has also been described by other authors[1,3] as body-centred cubic with lattice parameter $a=0.498$ nm. Its unit cell contains two selenium atoms placed at the bcc lattice points and four silver atoms statistically distributed among the 42 interstitial sites.

Crystal structure data in the literature for the low-temperature (LT) semiconductor phases of Ag_2Se are contradictory. At temperatures below the transition point, the compound has been described as cubic, tetragonal, orthorhombic, triclinic and sometimes as monoclinic (Table 1) for specimens prepared using different methods and conditions. Wiegers[13] has determined a LT-Ag_2Se structure by X-ray powder methods and found an orthorhombic cell with space group $P2_12_12_1$, which is completely different from the structure described by Pinsker et al.[8]. It seems that other LT-Ag_2Se phases are only stable in thin films. Y. Saito et al.[18] investigated Ag_2Se films and found that tetragonal, orthorhombic and triclinic modifications exist as distinct LT phases. The crystal structures of the orthorhombic and triclinic phases of Ag_2Se have been determined from observed structure images and their computer simulated images by C. Kaito et al.[21]. They found space group P222 for the orthorhombic and P1 for the triclinic cell, P422 is proposed for the tetragonal form.

* Institute for Inorganic Chemistry, University of Zürich, Winterthurerstrasse 190, CH-8057 Zürich, Switzerland.

Table 1. Literature data for LT-Ag_2Se phases (not complete)

Symmetry	Lattice constants	Investigation method	Ref.
Tetragonal	$a=b=0.706$ nm $c=0.498$ nm	Electron diffraction as $f(T)$	[3]
Tetragonal, after heating and cooling cycle	$a=b=0.498$ nm $c=0.478$ nm		
Tetragonal	$a=b=0.706$ nm $c=0.498$ nm	X-ray diffraction	[4]
Not tetragonal	—	X-ray diffraction	[5]
Orthorhombic	$a=0.434$ nm $b=0.711$ nm $c=0.779$ nm	X-ray diffraction	[6]
Orthorhombic	$a=0.705$ nm $b=0.433$ nm $c=0.782$ nm	Electron diffraction	[7]
Orthorhombic $P222_1$	$a=0.705$ nm $b=0.433$ nm $c=0.785$ nm	Electron diffraction	[8]
Orthorhombic	$a=0.434$ nm $b=0.707$ nm $c=0.775$ nm	X-ray diffraction	[9]
Orthorhombic	$a=0.705$ nm $b=0.432$ nm $c=0.782$ nm	Electron diffraction	[10]
Orthorhombic	$a=0.705$ nm $b=0.783$ nm $c=0.433$ nm	Electron diffraction as $f(T)$	[11]
Orthorhombic	$a=0.705$ nm $b=0.425$ nm $c=0.806$ nm	Electron diffraction	[12]
Orthorhombic $P2_12_12_1$	$a=0.433$ nm $b=0.706$ nm $c=0.776$ nm	X-ray diffraction	[13]
Tetragonal (metastable)	$a=b=0.706$ nm $c=0.498$ nm	Electron diffraction as $f(T)$	[14]
Orthorhombic	$a=0.705$ nm $b=0.785$ nm $c=0.433$ nm		
Orthorhombic	$a=0.705$ nm $b=0.785$ nm $c=0.433$ nm	Electron diffraction	[15]
Monoclinic	$a=0.423$ nm	Electron diffraction	

	a=0.691 nm c=0.787 nm β=99°35′		
Orthorhombic	a=0.434 nm b=0.706 nm c=0.776 nm	Electron diffraction as $f(T)$	[16]
Pseudo orthorh., triclinic	a=0.70 nm b=0.78 nm c=0.43 nm α=92° β=91.5° γ=92°	Electron diffraction	[1]
Pseudo orthorh., tric.	Lattice parameters as in [1]	Electron diffraction	[17]
Cubic fcc, metastable Orthorhombic	a=0.565 nm a=0.434 nm b=0.706 nm c=0.776 nm	Electron diffraction	[18]
Tetragonal (with excess Ag) Orthorhombic Triclinic Monoclinic (≥45°C) 	a=b=0.706 nm c=0.498 nm a=0.706 nm b=0.780 nm c=0.434 nm a=0.699 nm b=0.779 nm c=0.430 nm α=92° β=91.5° γ=92° a=0.691 nm b=0.787 nm c=0.423 nm α=99.58°	Electron diffraction	[19]
Orthorhombic, triclinic Tetragonal, P422 	Lattice param. as [21] a=b=0.706 nm c=0.498 nm	Electron diffraction Not indicated	[20]
Orthorhombic, P222 Triclinic, P1 	a=0.706 nm b=0.780 nm c=0.434 nm a=0.70 nm b=0.78 nm c=0.43 nm α=92° β=91.5° γ=92°	Electron diffraction HREM, computer sim.	[21]

The only known compound in the system Au-Ag-Se is Ag_3AuSe_2, a mineral called "fischesserite", isostructural to Ag_3AuTe_2 (petzite), space group $I4_132$[22] with lattice parameter $a=0.997$ nm. Tavernier et al.[24] performed differential thermoanalytical investigations on silver-gold(I)-chalcogenides. They found that silver in Ag_2Se can be substituted by gold in aqueous solution of $Au(S_2O_3)_2^{3-}$ up to 25 at% leading to the composition $AuAg_3Se_2$, determined earlier by Messien et al.[23].

In our investigations we produced thin epitaxially grown silver and mixed silver/gold films on (100) cleaved KCl faces and studied the structural changes after selenation.

EXPERIMENTAL

Thin films of $Au_xAg_{2-x}Se$ were prepared by vacuum deposition of the compo-

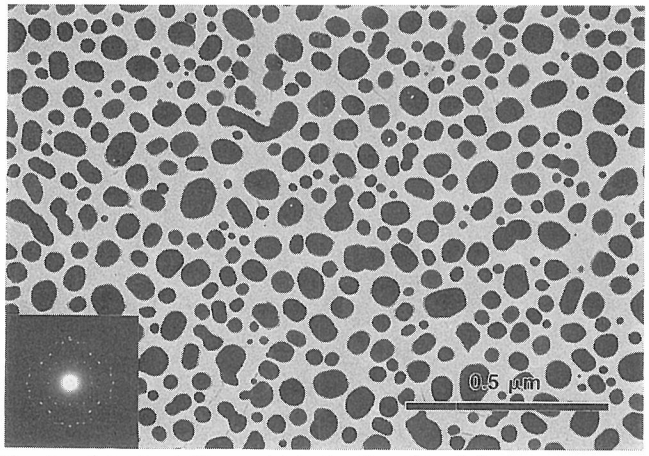

Fig. 1. Selenized 15 nm thick Ag-film (Ag_2Se) deposited onto (100) cleavage face of KCl at a substrate temperature of 300°C. Inset: SAED pattern. Lattice orientation: $[010]_{tetr.}//[001]_{Ag}$.

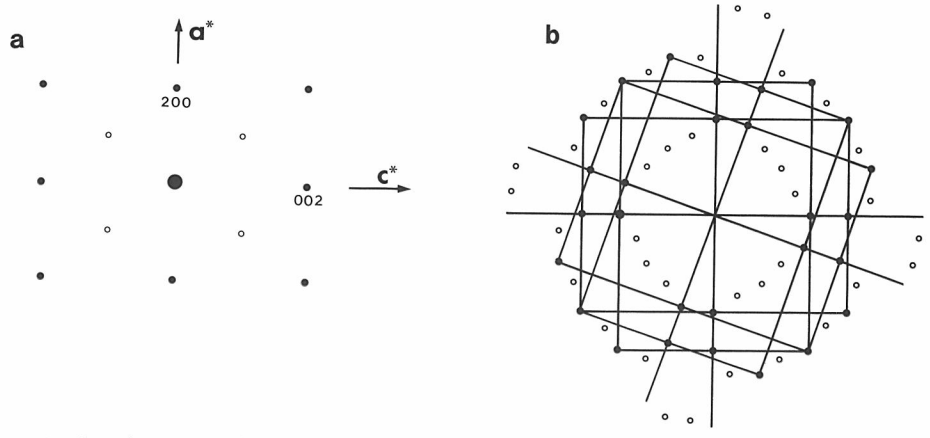

Fig. 2. a) Basic diffraction pattern of the tetragonal Ag_2Se-phase. b) Superposition of four orientations; rotations by 19.5, 90 and 109.5°.

nents on KCl crystals, which were (001)-cleaved in air and then immediately placed in a chamber to be evacuated down to $<6.5 \cdot 10^{-5}$ Pa. Silver or silver/gold was deposited onto the preheated KCl surface (300°C for four hours) from a tungsten boat at a deposition rate of about 1.2–1.5 nm/min. Rate and film thickness were measured with an oscillating quartz crystal microbalance. Selenium was evaporated onto the Ag- or Au/Ag-films immediately after the substrate temperature had reached 210–230°C (measured with a constantan-Ni thermocouple) or after cooling to room temperature (to take out samples) and heating up again to 200°C at a deposition rate between 1.2–20 nm/min. Films were annealed at the same temperature for 15 min (annealing at higher temperatures leads to decomposition) and then cooled to room temperature. These layers were covered with a 10 nm thick carbon layer to stabilize the small crystallites, wet stripped in bidis-

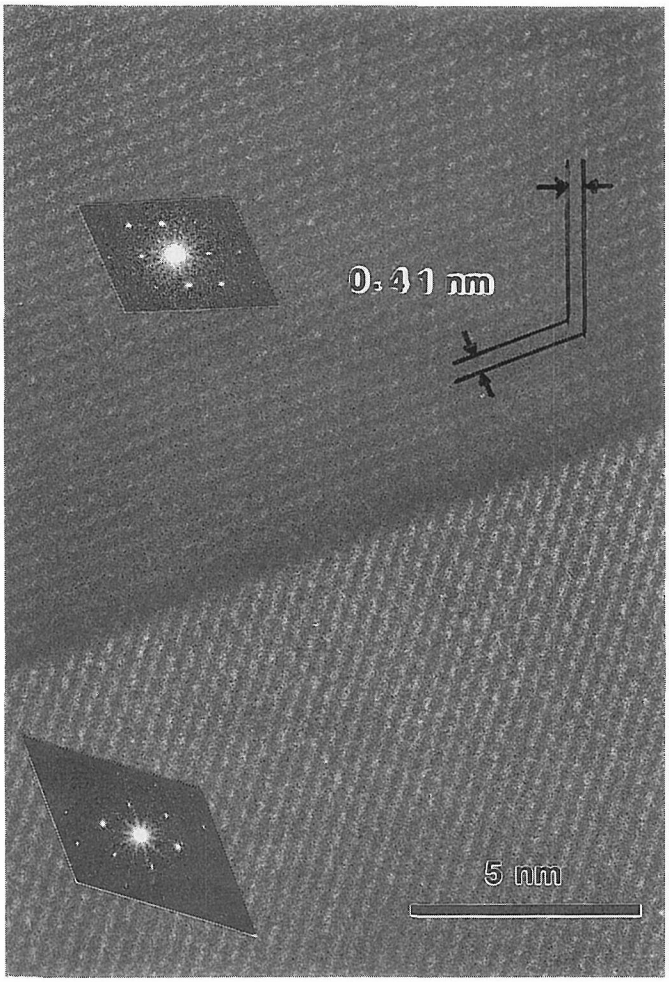

Fig. 3. HREM image of a twinned tetragonal Ag_2Se crystal, [010] zone axis. Fringes with 0.41 nm correspond to the (101) planes. Inset; Optical diffraction patterns.

tilled water and collected on holey carbon films on copper specimen grids. The composition of the Au/Ag-layers is not identical with the weighted proportion of the metals as shown by quantitative electron microprobe analysis (ARL electron microprobe). Electron microscopic observations were performed within a JEOL 200CX electron microscope operating at 200 kV (c_s=1.2 mm) or within a Hitachi HU-125S EM operating at 75 kV for low magnification images and selected area electron diffraction (SAED). Simulated images and electron diffraction patterns for various trial models were calculated by the EMS programs[25]. Optical diffraction patterns were obtained with a laser diffractometer, built according to Ref. 26, 27.

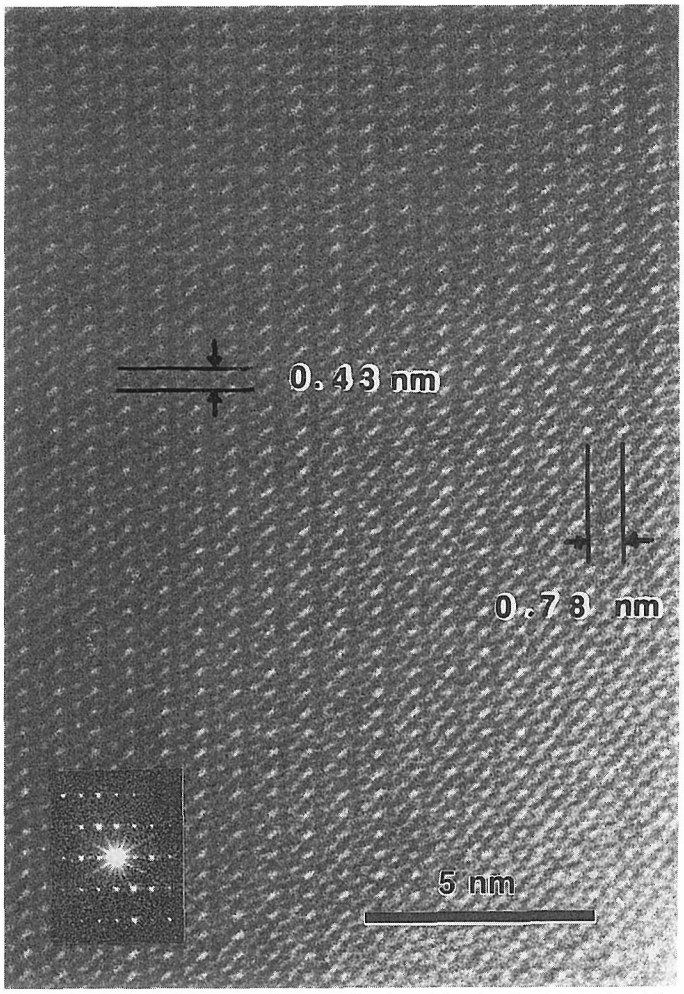

Fig. 4. HREM image of an orthorhombic Ag_2Se crystal with the [100] direction parallel to the film normal. Fringes with 0.78 and 0.43 nm correspond to the (010) and (001) planes. Inset: Optical diffraction pattern.

RESULT AND DISCUSSION

Thin Films of Pure Ag_2Se

Epitaxially grown thin silver films were obtained in two different ways: evaporation of a 2 nm Ag-layer at T_{KCl}: 300°C for prenucleation followed by a second evaporation of silver (10–13 nm) either at T_{KCl}: 300°C or after cooling the substraet to room temperature. Selenation of these silver films at T_{KCl}: 230°C leads to Ag_2Se-layers whose SAED patterns indicate either a mixture of triclinic, orthorhombic and tetragonal phases or show large areas with d-spacings corresponding to the tetragonal cell (Fig. 1).[3] Lattice orientation: $[010]_{tetr.}//[001]_{Ag}$. The continuous silver film has broken up into islands, but is still oriented. The

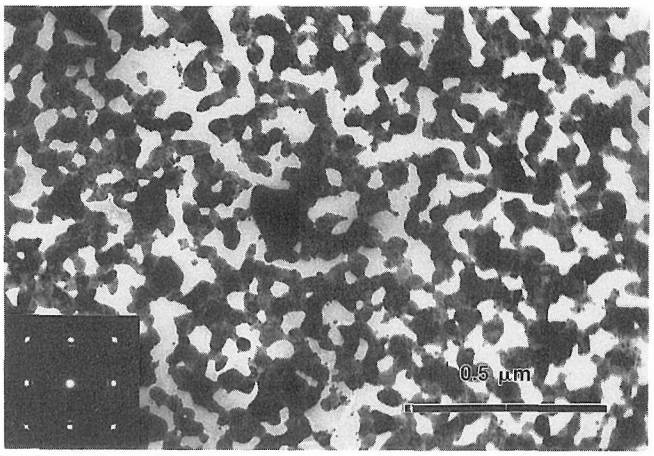

Fig. 5. Epitaxially grown, continuous Au/Ag-film (x=0.5), 15 nm thick, T_{KCl}: 300°C.

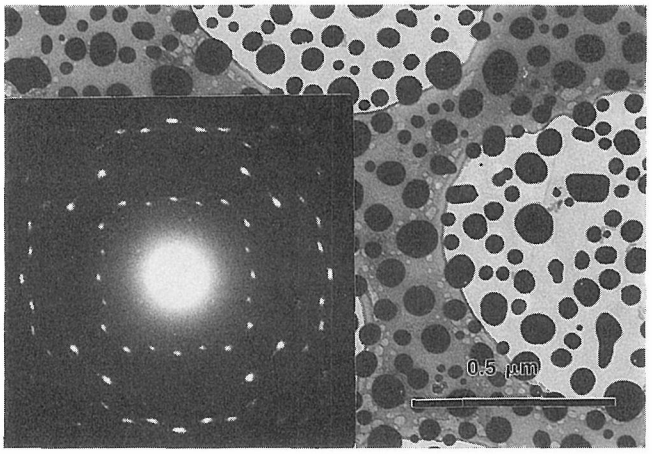

Fig. 6. Au/Ag-film (as in Fig. 5) after reaction with Se vapour at T_{KCl}: 200°C, annealing at the same temperature for 1 hr and cooling. The film has broken up into islands, but is still oriented. Inset: SAED pattern.

basic electron diffraction pattern consists of rectangular arrays of spots with edges in the ratio of $1:\sqrt{2}$. The additional spots are due to rotations of the basic pattern by 19.5°, 90° and 109.5° as a consequence of corresponding 90° rotations of crystallites and twinning on (101) planes (Fig. 2), as discussed by Dhere et al.[12] for HT-Ag_2Se. All HREM images observed belong to the [100] zone axis of twinned tetragonal Ag_2Se crystals (Fig. 3), as proved by optical diffraction patterns. Among the tetragonal crystals one could find occasionally singular orthorhombic particles, which do however not contribute to the overall SAED pattern (Fig. 4).

Thin Films of $Au_xAg_{2-x}Se$ ($x=0.1$-0.5)

Based on our results on the preparation of thin epitaxially grown mixed Ag/

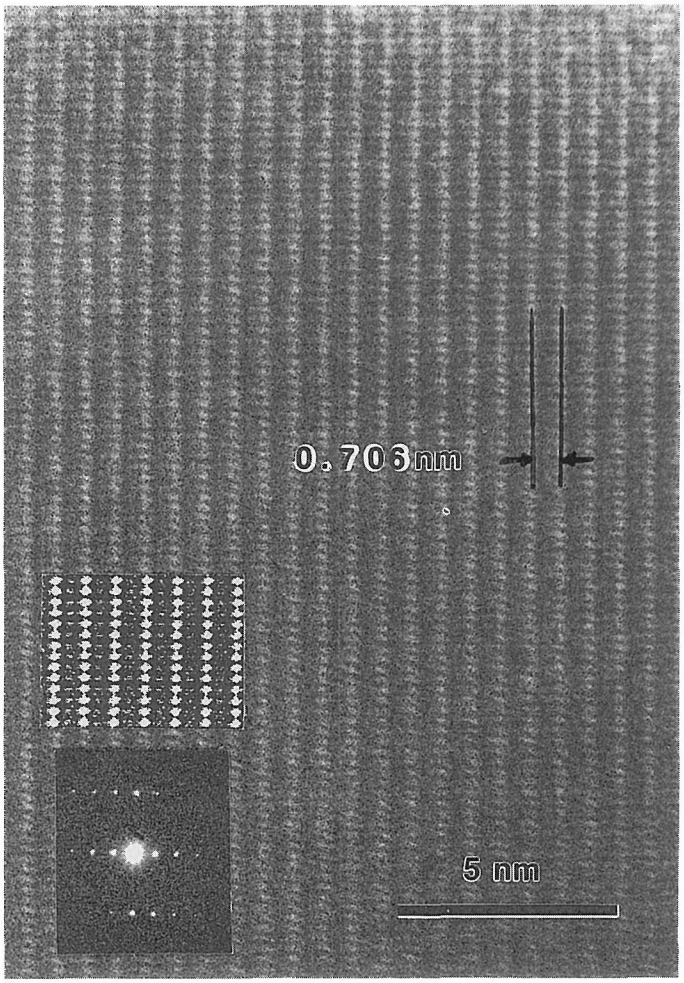

Fig. 7. Pseudotetragonal $Au_xAg_{2-x}Se$ ($x=0.5$), [100] zone axis. Fringes with 0.706 nm correspond to (001) planes. Insets: Optical diffraction pattern and simulated image (200 kV, Defocus: −72 nm, Thickness: 14 nm).

Au-layers[28], we have studied the reaction of such films with selenium vapour. Fig. 5 shows a low magnification electron micrograph and a corresponding selected area electron diffraction (SAED) pattern of a mixed Ag/Au-layer (15 nm thick), grown on (100) KCl faces at a substrate temperature of 300°C with parallel lattice orientation relative to the silver. The content of gold in the continuous film lies between 15 and 20 at %, as revealed by quantitative electron microprobe analysis for thicker layers (25 nm). After reaction with Se vapour at T_{KCl}: 200°C (until the microbalance with its quatz crystal held at room temperature indicated a thickness of 15 nm for fully selenized samples), the film has broken up into islands as illustrated by Fig. 6. Its SAED pattern shows d-spacings corresponding to the tetragonal cell with additional spots due to rotations and twinning (see Fig. 2), a

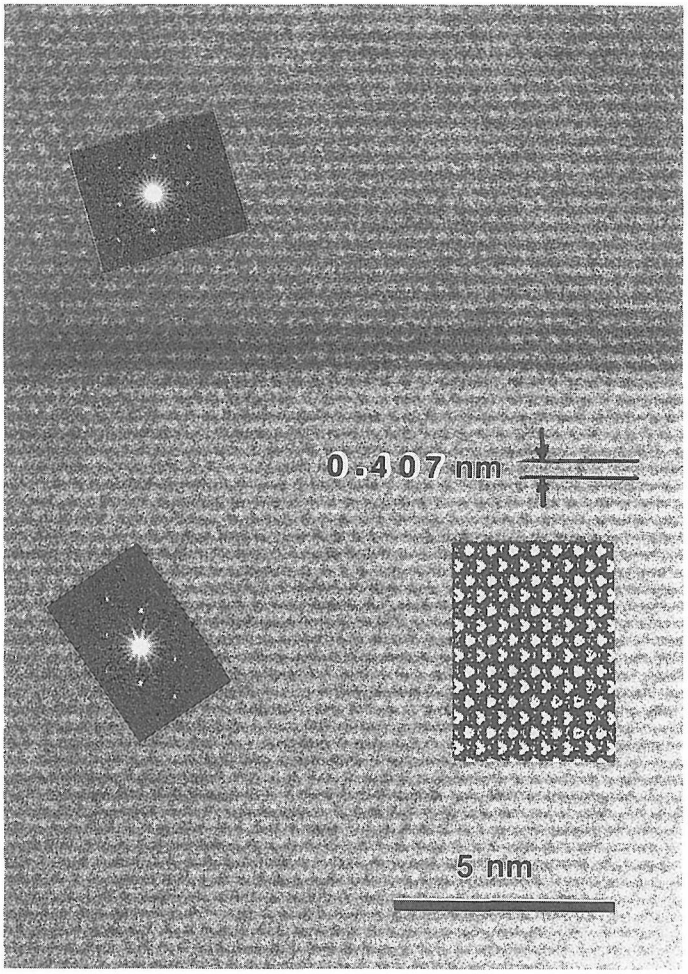

Fig. 3. Twinned pseudotetragonal $Au_xAg_{2-x}Se$ crystal, [001] zone axis. Fringes with 0.407 nm corresdond to (110) planes. Insets: Optical diffraction pattern and simulated image (200 kV, Defocus: −77 nm, Thickness: 14 nm).

consequence of the deposition temperature being higher than the transition point; the bcc HT-Ag_2Se phase twins on (211) planes[1,16] and then induces twinning on (101) planes in the tetragonal phase at room temperature. This behaviour is different from that observed for triclinic pure Ag_2Se.[29]

Variation of the Au content (5–25 at %) reproducibly yields electron diffraction patterns with tetragonal symmetry as shown in Fig. 4 and 5 over the entire samples. In high resolution electron microscopic observations of these layers, three different types of crystallites could be observed, illustrated by Fig. 7–9 (unit cell of[21]). An example of the frequently observed crystal defects is shown in Fig. 10. Shiojiri et al.[20] proposed as space group P422 for the tetragonal

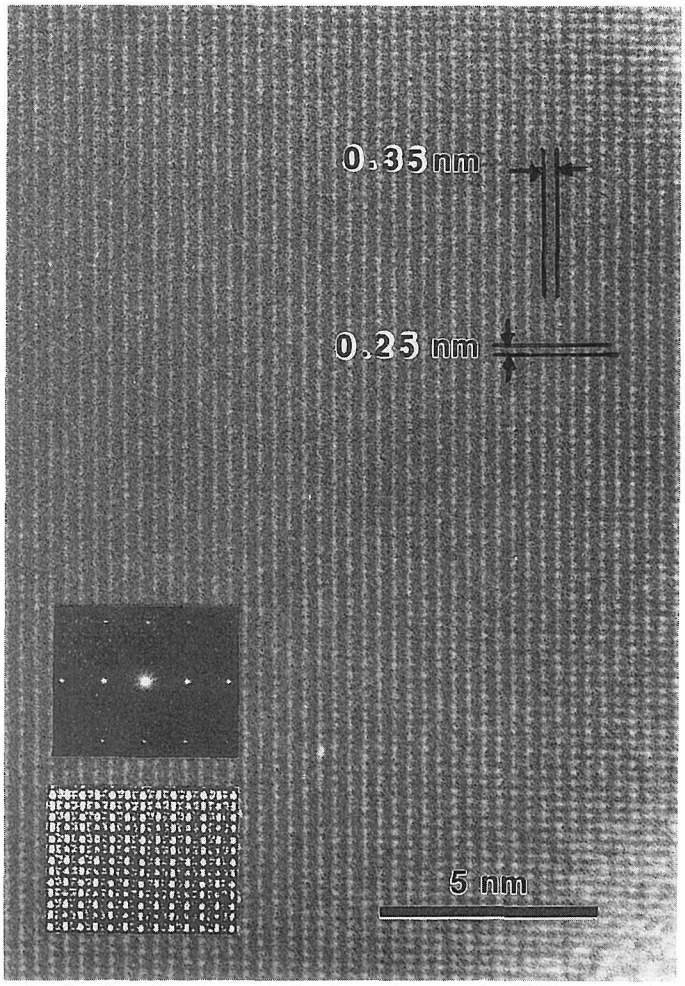

Fig. 9. Pseudotetragonal $Au_xAg_{2-x}Se$ crystal, [001] zone axis. Fringes with 0.353 and 0.25 nm correspond to (200) and (020) planes. Insets: Optical diffraction pattern and simulated image (200 kV, Defocus: −92 nm, Thickness: 14 nm).

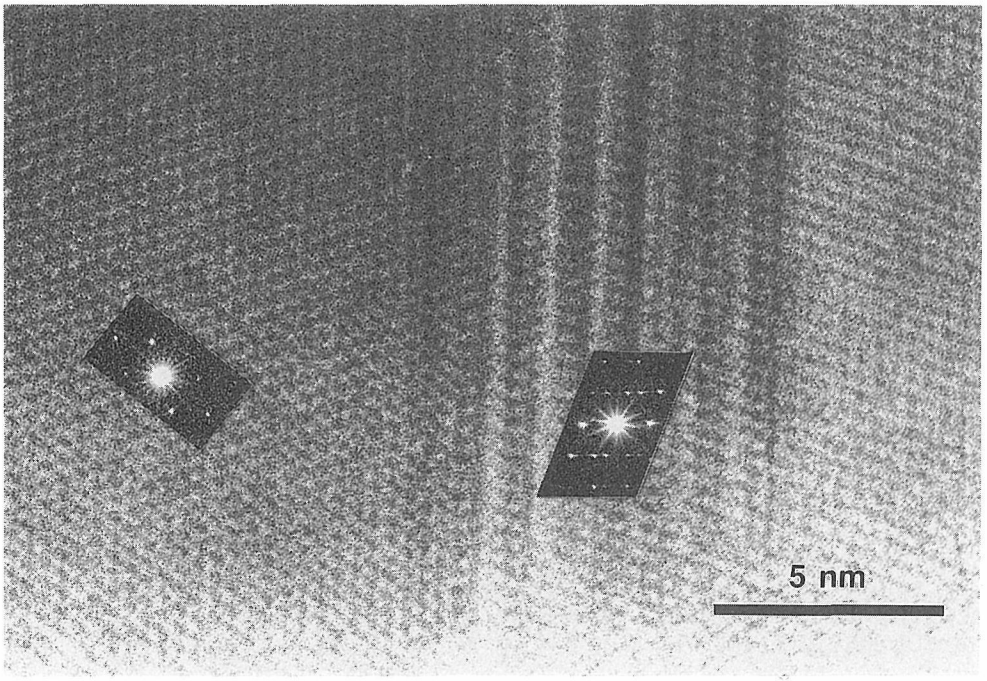

Fig. 10. Example for the frequently observed crystal defects in $Au_xAg_{2-x}Se$ crystals, which are not yet fully understood. Insets: Optical diffraction patterns.

LT-Ag_2Se, but simulated images and calculated electron diffraction patterns using the coordinates given for Se and Ag do not explain our electron micrographs. Calculations on various trial models, taking into consideration reasonable bond distances, only lead to a satisfactory agreement for a pseudotetragonal unit cell with the monoclinic space group P2, with $a=c=0.706$ nm, $b=0.498$ nm, $\beta=90°$, $Z=4$. The Se atoms are placed in face centering positions of the pseudotetragonal lattice and the Ag atoms have the following coordinates: 0.84, 0, 0.34; 0.16, 0, 0.66; 0.3, 0.25, 0.25; 0.7, 0.25, 0.75; 0.36, 0.5, 0.64; 0.64, 0.5, 0.36; 0.2, 0.75, 0.25; 0.8, 0.75, 0.25.

The Ag-Ag distances in thin Ag_2Se films of space group $P222_1$ determined by Pinsker et al.[8] are short, ranging from 0.261 to 0.282 nm (in metallic silver: 0.289 nm). This structure contains Ag-Se-Ag-Se chains with short Ag-Se distances of 0.254 nm. For the structure described by Wiegers[13] in space group $P2_12_12_1$ the shortest Ag-Ag distance is 0.293 nm, the shortest Ag-Se bond 0.262 nm. The model proposed by Shiojiri et al.[20] (tetragonal, space group P422) contains four extremely short Ag-Ag contacts of 0.255 nm. The shortest Ag-Ag distance in our model is 0.261 nm similar to Pinsker et al.[8], the other Ag-Ag distances range between 0.28 and 0.329 nm. Assuming a minimum Ag-Se contact of 0.262 nm, we performed our model calculations by distributing the Ag atoms into the largest interstices (42 possibilities for Ag atoms).

REFERENCES

(1) R. de Ridder and S. Amelinckx, *phys. stat. sol.* (*a*), **18**, 99 (1973).
(2) P. Ralphs, *Z. phys. Chem.* B, **31**(3), 157 (1936).
(3) A. Boettcher, G. Haase and H. Treupel, *Z. angew. Phys.*, **7**(10), 478 (1955).
(4) P. Junod, *Helv. Phys. Acta*, **32**, 367 (1959).
(5) W. Sander, *Z. Phys.*, **159**, 456 (1960).
(6) J.B. Conn and R.C. Taylor, *J. Electrochem. Soc.*, **10**, 977 (1960).
(7) C. Ching-liang and Z.G. Pinsker, *Sov. Phys.-Crystallogr.*, **7**(1), 52 (1962).
(8) Z.G. Pinsker, C. Ching-liang, R.M. Imanov and E.L. Lapidus, *Sov. Phys.-Crystallogr.*, **10**(3), 225 (1965).
(9) A.V. Novoselova, Zh.G. Shleifman, V.P. Zlomanov and R.K. Sloma, *Inorg. Mater*, **3**, 1010 (1967).
(10) S.K. Sharma, *J. Mat. Science*, **4**, 189 (1969).
(11) G.A. Efendiev, I.R. Nuriev, R.B. Shafizade, *Sov. Phys.-Crystallogr.*, **14**(5), 787 (1970).
(12) N.G. Dhere and A. Goswami, *Thin Solid Films*, **5**, 137 (1970).
(13) G.A. Wiegers, *Am. Mineral.*, **56**, 1882 (1971).
(14) I.R. Nuriev and R.B. Shafizade, Izv. Akad. Nauk Azerb. SSR, Ser. Fiz.-Tekh. Mat. Nauk (2), 13 (1972).
(15) L.R. Nuriev, R.M. Sultanov and F.I. Aliev, Izv. Akad. Nauk Azerb. SSR, Ser. Fiz.-Tekh. Mat. Nauk (1), 52 (1973).
(16) L.V. Constantinescu and A. Ichimesca, *Rev. Roum. Phys.*, **18**, 1197 (1973).
(17) J.R. Günter, N. Uyeda and E. Suito, *J. Cryst. Growth*, **28**, 209 (1975).
(18) L.V. Constantinescu, *Thin Solid Films*, **32**, 333 (1976).
(19) Y. Saito, M. Sato and M. Shiojiri, *Thin Solid Films*, **79**, 257 (1981).
(20) M. Shiojiri, C. Kaito, S. Sekimoto, K. Teranishi and N. Nakamura, Electron Microscopy 1982 Vol. 2 Material Sciences p. 207, 1982 DGEeV D-6000 Frankfurt/Main.
(21) C. Kaito, N. Nakamura, K. Teranishi, S. Sekimoto and M. Shiojiri, *phys. stat. sol.* (*a*), **71**, 109 (1982).
(22) Z. Johan, P. Picot, R. Pierrot and M. Kvacek, *Bull. Soc. Fr. Minéral. Critallogr.*, **94**, 381 (1971).
(23) P. Messien and M. Baiwir, *Bull. Soc. Roy. Sc. Liège*, **35**(3), 234 (1966).
(24) B.H. Tavernier, J. Vervecken, P. Messien and M. Baiwir, *Z. anorg. allg. Chem.*, **356**, 77 (1967).
(25) P.A. Stadelmann, *Ultramicroscopy*, **21**, 131 (1987).
(26) B.E.P. Beeston, R.W. Horne and R. Markham, Electron Diffraction and Optical Diffraction Techniques, ed: A.M. Glauert, North-Holland Publ. Comp., Amsterdam 1973.
(27) J.C.H. Spence, Experimental HREM, ed: C.E.H. Bawn, H. Frölich, P.B. Hirsch and N.F. Mott Clarendon Press, Oxford 1981, p. 275.
(28) P. Keusch, J.R. Günter and R. Bauer, Electron Microscopy 1986, Vol. 2, p. 1379, The Japanese Society of Electron Microscopy, Tokyo, Japan 1986.
(29) J.R. Günter, N. Uyeda and E. Suito, Electron Microscopy 1974, Vol. 1, p. 526, The Australian Academy of Science, Canberra, Australia 1974.